

# Oxidative stress and mitochondrial dysfunction of retinal ganglion cells injury exposures in long-term blue light

Ke-Xin Guo<sup>1</sup>, Chen Huang<sup>2</sup>, Wei Wang<sup>3</sup>, Pei Zhang<sup>3</sup>, Ying Li<sup>3</sup>, Zi-Yuan Liu<sup>3</sup>, Min-Shu Wang<sup>3</sup>

<sup>1</sup>Peking University Third Hospital, Beijing 100191, China

<sup>2</sup>Medical Research Center, Peking University Third Hospital, Beijing 100191, China

<sup>3</sup>Department of Ophthalmology, Peking University Third Hospital, Beijing 100191, China

**Correspondence to:** Chen Huang. Medical Research Center, Peking University Third Hospital, 49 North Garden Road, Haidian District, Beijing 100191, China. candyhuang719@hotmail.com; Wei Wang. Department of Ophthalmology, Peking University Third Hospital, 49 North Garden Road, Haidian District, Beijing 100191, China. puh3\_ww@bjmu.edu.cn

Received: 2020-06-19 Accepted: 2020-07-14

## Abstract

• **AIM:** To investigate the phototoxic effect of long-term excessive narrow-band blue light in staurosporine-induced differentiated retinal ganglion cells-5 (SSRGC-5).

• **METHODS:** SSRGC-5 cells were divided into two groups, blue light group (BL group) and control group. Cell viability was assessed by using CCK-8 assay. Metabolic profile analysis was performed by using Seahorse extracellular flux analyzer. Mitochondria ultrastructure were studied via transmission electron microscope (TEM). Mitochondria contents and oxidative stress was evaluated by flow cytometry. Western blotting was performed to monitor the changes in mitogen-activated protein kinases (MAPK) pathway and PI3K/AKT pathway.

• **RESULTS:** Blue light caused morphological changes of SSRGC-5 cells. The cell viability was significantly decreased from 3h in BL group. Intercellular ROS and mitochondrial superoxide levels were increased following blue light exposure. Metabolic profiling identified blue light induced SSRGC-5 cells to have severely compromised mitochondrial function. This was accompanied by impaired mitochondrial ultrastructure and remodeling, increased expression of the mitochondrial related proteins, and increased glycolysis as compensation. Moreover, the results showed that blue light induced higher expression of p-p38, p38, p-JNK, p-ERK, p-c-Jun, c-Jun, and p-AKT.

• **CONCLUSION:** These findings indicate that excessive narrow-band blue light induces oxidative stress and

mitochondrial metabolic remodeling dysregulate in SSRGC-5 cells. Activated MAPK and AKT signaling pathways are involved in this process.

• **KEYWORDS:** blue light; retinal ganglion cell; oxidative stress; mitochondria metabolism; mitochondria abnormalities; mitogen-activated protein kinases; AKT

**DOI:10.18240/ijo.2020.12.03**

**Citation:** Guo KX, Huang C, Wang W, Zhang P, Li Y, Liu ZY, Wang MS. Oxidative stress and mitochondrial dysfunction of retinal ganglion cells injury exposures in long-term blue light. *Int J Ophthalmol* 2020;13(12):1854-1863

## INTRODUCTION

Blue light, a major component of visible light with a wavelength of 420-490 nm, may contribute to the pathogenesis of age-related macular degeneration and vision loss<sup>[1]</sup>. Previous research regarding light damage has focused on retinal pigment epithelium (RPE) and photoreceptor cells; however, light-induced retinal ganglion cells (RGCs) injury has gained increasing attention in recent years.

RGCs are important components of the retina. As is the case for other nerve cells, damage to RGCs is irreversible. Intraocular axons of RGCs are unmyelinated, and can be directly affected by excessive light<sup>[2]</sup>. Different results explaining the mechanism of blue light injury in RGCs have been published. Some reports state that the apoptotic pathway is involved via an increase in caspase-3 and Bax protein levels. In addition, necroptosis participates in RGC-5 cell injury after blue light exposure through different signaling pathways, including those mediating apoptosis inducing factor (AIF) activation<sup>[3]</sup>. Both apoptosis and necroptosis are related to mitochondria, indicating that mitochondria play an important role in blue light injury<sup>[4-5]</sup>.

Mitochondria, as cellular powerhouses, play an essential role in energy metabolism and are densely packed in RGCs to satisfy the high energy demand of the cells<sup>[6]</sup>. Various components of mitochondria such as cytochrome oxidase and cytochrome P450 have absorption to light around 400-450 nm, which makes mitochondria a potential target of light injury. To maintain homeostasis, mitochondria form elongated

tubules that continually undergo fission and fusion<sup>[7]</sup>. When this equilibrium is imbalanced, mitochondria lose their characteristic shape and exhibit abnormal functions. However, few reports have described alterations in energy metabolism and mitochondrial remodeling in RGCs with blue light-induced injury in detail.

Although information concerning the toxicity of blue light to RGCs is limited, several studies have reported that oxidative stress might be a key toxicity mechanism related to retinal cells exposure to blue light<sup>[8]</sup>. Increased reactive oxygen species (ROS) drives cellular cytotoxicity or apoptosis by modulating downstream signaling pathways, including the mitogen-activated protein kinases (MAPK) and AKT pathway<sup>[9]</sup>. Blue light-induced damage to RGC-5 cells has been reported to be related to ROS-mediated pathways, but the mechanism relevant to RGC-5 cell damage remains uncertain<sup>[10]</sup>. Recently, staurosporine-induced differentiated RGC-5 (SSRGC-5) cells have been widely used in research on RGC phototoxicity<sup>[11]</sup>. Therefore, the current study aimed to investigate mitochondrial energy metabolism and the underlying mechanism in SSRGC-5 cells exposed to blue light.

## MATERIALS AND METHODS

**Cell Culture and Treatments** The RGC-5 cell line was purchased from Fudan Cell Culture Center (Shanghai, China) and cultured in low glucose Dulbecco's modified Eagle's medium (DMEM; Gibco, USA) containing 10% fetal bovine serum (FBS; Biochrom AG, Germany) under a humidified atmosphere of 5% CO<sub>2</sub> at 37°C. RGC-5 cells were passaged by trypsinization in 0.25% trypsin-EDTA (Gibco, USA) every 2-3d.

RGC-5 cells were seeded onto plates and cultured under a humidified atmosphere of 5% CO<sub>2</sub> at 37°C for 4h to promote differentiation. The medium was subsequently replaced with serum-free, phenol red-free DMEM (Gibco, USA) containing 200 nmol/L staurosporine (Beyotime, China) and incubated for 24h. Following 24h of differentiation, the medium was replaced with phenol red-free DMEM.

Narrow-band blue light (main wavelength, 464 nm; peak wavelength, 456 nm; half bandwidth, 27 nm) illumination was applied as described previously<sup>[10-11]</sup>. Cells were exposed to blue light for different time periods (0, 1, 3, 6, 12, 18, and 24h) at an output power of 5 W/m<sup>2</sup> (the intensity of 1370 lx) at 37°C in a humidified atmosphere containing 5% CO<sub>2</sub>. Unexposed, serum-deprived SSRGC-5 cells served as a control.

**Cell Viability Assay** Cell viability was assessed using a CCK-8 kit (Dojindo Laboratories, Kumamoto, Japan). RGC-5 cells were seeded in 96-well plates at a density of 10 000 cells/well and differentiated by using staurosporine. After incubation for 24h, the cells were exposed to blue light for different time periods. Then 10 mL CCK-8 solution was added to each well. The cells were incubated at 37°C for 2h. The absorbance was

detected at 450 nm using an enzyme-linked immunosorbent assay (ELISA) reader (BioTek, USA). All experiments were performed in triplicate.

## Hoechst 33342 and Propidium Iodide Co-staining Assay

The rate of cell death after blue light exposure was detected by using costaining with Hoechst 33342 (Sigma-Aldrich, USA) and PI (Sigma-Aldrich, USA). Cells were stained with 5 g/mL Hoechst 33342 for 10min in the dark at 37°C. Then, PI was added to the culture medium at a final concentration of 5 g/mL and incubated for 10min at 4°C. The morphology of stained nuclei/DNA was visualized under a Nikon TE2000-S fluorescence microscope (Tokyo, Japan).

**Metabolic Analysis** RGC-5 cells were seeded in Seahorse Bioscience XFp cell culture miniplates at a density of 18 000 cells/well. Following differentiation, cells were exposed to blue light as previously described. Cells were washed three times with Seahorse XF assay medium and preincubated in the same medium at 37°C for 1h in a humidified incubator without CO<sub>2</sub>. The assay medium consisted of Seahorse XF base medium (Seahorse Bioscience, USA) supplemented with 2 mmol/L L-glutamine, 1 mmol/L pyruvate, and 10 mmol/L glucose (Sigma-Aldrich, USA). The energy phenotype and Mito Stress tests were performed according to the manufacturer's protocols.

In the energy phenotype test, we evaluated the oxygen consumption rate (OCR) and extracellular acidification rate (ECAR), which reflect the mitochondrial aerobic respiration and glycolysis levels, respectively. First, the baseline OCR and ECAR were measured without any inhibitors, reflecting basal metabolism. Following sequential addition of oligomycin (inhibits oxygen consumption) and FCCP [uncouples oxidative phosphorylation (OXPHOS)], both the OCR and ECAR were increased as the cells entered a stressed state.

In the Mito Stress test, the baseline OCR was measured first, and oligomycin and FCCP were then added sequentially. Subsequently, non-mitochondrial respiration (non mito) was determined by the addition of the complex I and III inhibitors rotenone and antimycin A, respectively. The OCR values were measured three times at each time point. Metabolic parameters were calculated using the OCR value: basal respiration (baseline OCR reading minus non-mitochondrial respiration), proton leak-linked respiration (the minimal reading after oligomycin addition but prior to FCCP addition minus non-mitochondrial respiration), ATP-linked respiration (basal respiration minus proton leak-linked respiration); maximal respiratory capacity (maximal uncoupled respiration minus non-mitochondrial respiration), spare respiratory capacity (maximal respiration minus non-mitochondrial respiration).

**Flow Cytometry Analysis** Intracellular ROS and mitochondrial superoxide formation in RGC-5 cells were

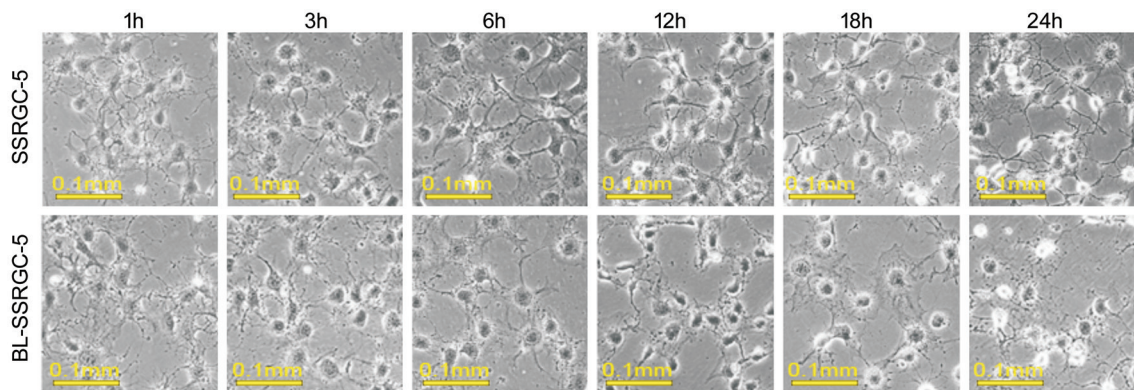


**Figure 1** Long-term excessive narrow-band blue light exposure caused morphological changes in SSRGC-5 cells.

determined separately using dichlorodihydrofluorescein diacetate (DCFH-DA; Beyotime, China) and MitoSox™ Red (Invitrogen, USA). MitoTracker® Green (Beyotime, China) was applied to measure the mitochondrial content. Following the blue light exposure period, cells were incubated with the different dyes according to the manufacturers' protocols. Subsequently, cells were rinsed twice in PBS and maintained in prewarmed phenol red-free DMEM. Fluorescence intensity was measured using a FACSCalibur cytofluorimeter (BD Bioscience, USA). For each analysis, a total of 10 000 events were recorded by flow cytometry. All experiments were performed in triplicate.

**Transmission Electron Microscopy** SSRGC-5 cells were harvested using 0.25% trypsin-EDTA, washed three times in PBS, and fixed in 4.0% glutaraldehyde in PBS overnight. Cells were subsequently embedded in epoxy resin, and ultrathin sections (50-70 nm) were collected on copper grids. Counterstaining was performed with aqueous uranyl acetate and phosphotungstic acid (sequentially; 1h each) followed by Reynolds' lead citrate (20min). Cells were examined on a transmission electron microscope (JEM 1010; JEOL).

**Western Blotting Analysis** Cells were harvested in RIPA buffer (Applygen Technologies, China) supplemented with phosphatase and protease inhibitors. The protein concentration was measured using a BCA assay kit (Applygen Technologies, China). Protein samples were separated on SDS-PAGE gels (Bio-Rad Laboratories, USA) and subsequently transferred to nitrocellulose membranes using a Trans-Blot Turbo Blotting System (Bio-Rad Laboratories, USA). The membranes were blocked in 5% skim milk for 1h at room temperature and probed overnight at 4°C with the following primary antibodies against: HO-1, OPA1, Fis1, Drp1, p38, p-p38 (phospho-Y182), ERK1/2, p-ERK1/2 (phospho-T202/Y204), JNK1/2/3, p-JNK1/2/3 (phospho-T183/Y185), c-Jun, p-c-Jun (phospho-S73), PI3K p85 $\alpha$ , p-PI3K p-p85 $\alpha$  (phospho-Tyr607), AKT, p-AKT (phospho-T308), and  $\beta$ -actin (Bioworld, USA). After washing, the membranes were incubated with the appropriate HRP-conjugated secondary antibodies (Golden

Bridge Biological, China) at room temperature for 1h. The bound antibodies were visualized using the Enlight™ ECL system (Applygen Technologies, China), and the relative amount of each immunoblotted protein was quantified using the Image J software.

**Statistical Analysis** Data are expressed as the mean $\pm$  standard deviation (SD) of at least three independent experiments. Statistical analyses were performed using a Student's *t*-test. A value of  $P < 0.05$  was considered statistically significant.

## RESULTS

**Morphological Changes in SSRGC-5 Cells** The controlled SSRGC-5 cells were round bodies and surrounded by slender axon-like branches. These branches were clear and complete with a synapse-like expansion structure at the ends, which connected with each other. With the prolongation of culture time, a small number of SSRGC-5 cells became smaller and weakened attached from 12h. The floating cells slightly increased at 24h, and most of the cells still maintained the round cell bodies and axon-like structures.

As shown in Figure 1, long-term excess narrow-band blue light exposure induced significantly morphological changes after 6h, such as fragmented axons and smaller bodies. With the prolongation of exposure time, the number of cells with smaller cell bodies and aggravated axonal fragmentation increased. Several floating cells appeared due to diminished adherence. After 18 and 24h of exposure, masses of cells showed indistinct, broken, and fragmented axons, with the shrunken cell body. Floating cells were also further raised. The above results show that excessive narrow-band blue light exposure can cause morphological changes of SSRGC-5 cells in time dependent.

**Reduced Cell Viability in SSRGC-5 Cells** Under long-term excessive narrow-band blue light exposure, the cell viability of BL-SSRGC-5 cells (SSRGC-5 cells in BL group) were a significant decrease examined by CCK-8 assay. The damage were significantly from 3h, and aggravated with the duration of exposure ( $P < 0.05$ ; Figure 2A). Compared with SSRGC-5 cells

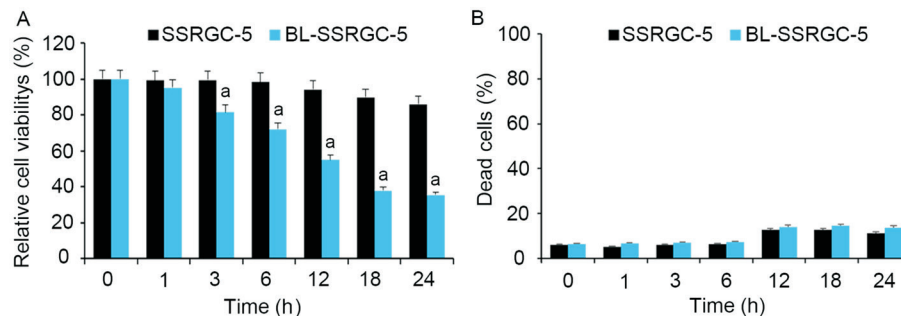


**Figure 2 Cell viability and death rates of SSRGC-5 cells after exposure to narrow-band blue light** A: Cell viability decreased significantly in the BL group; B: The rate of cell death did not differ after blue light exposure. <sup>a</sup> $P < 0.05$ .

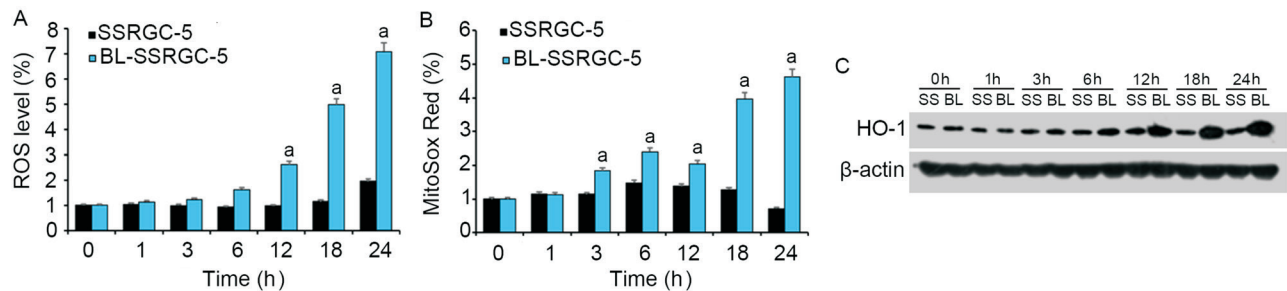


**Figure 3 Narrow-band blue light exposure induced oxidative stress in cells** A: DCF fluorescence, serving as an indicator of ROS generation, was significantly increased in the BL group; B: MitoSox™ Red fluorescence, serving as an indicator of mitochondrial superoxide production, was significantly increased in the BL group; C: The expression of the redox-sensitive protein HO-1 was notably increased after blue light exposure for 6, 12, 18, and 24h. <sup>a</sup> $P < 0.05$ .

at 0h (100%), BL-SSRGC-5 cell viability decreased to 37.70% after 18h and 35.26% at 24h. However, the cell viability of the control cells was a slight decrease from 12h and no significant difference.

Moreover, double staining with Hoechst 33342 and PI dyes was used to distinguish between dead and live cells (Figure 2B). No significant differences in the cell death rates were observed among the two groups with slightly increased from 12h after exposure. At the same time point, BL-SSRGC-5 cells were slightly higher than SSRGC-5 cells but no significant difference, indicating that SSRGC-5 cell death was not significant after 24h of excessive narrow-band blue light exposure.

**Accumulated Mitochondrial Oxidative Stress in SSRGC-5 Cells** Intracellular ROS and mitochondrial superoxide levels in cells were measured as an important biomarker for oxidative stress to determine the potential mechanism in the injurious effects of long-term excessive narrow-band blue light exposure. Results of fluorescence intensity of DCFH-DA by flow cytometry showed that the intercellular ROS levels were significantly increased following blue light exposure for 6, 12, 18, and 24h ( $P < 0.05$ ; Figure 3A).

Notably, after 3h-exposure, the levels of mitochondrial superoxide, indicated by MitoSox™ Red, significantly higher than the level of the control cells, and accumulated in time dependent. Enhanced fluorescence was observed in BL-

SSRGC-5 cells as compared with unexposed SSRGC-5 cells, with intensities of 161.23%, 161.02%, 147.79%, 308.70%, and 644.27% of the control at 3, 6, 12, 18, and 24h, respectively ( $P < 0.05$ ; Figure 3B).

HO-1, a rate-limiting enzyme in heme catabolism, plays a key role among the inducible antioxidant defenses. Western Blotting analysis showed a significant induction of HO-1 in blue light-exposed cells from 6h in comparison to unexposed cells (Figure 3C).

In summary, after excessive narrow-band blue light exposure, the level of mitochondrial oxidative stress in SSRGC-5 cells gradually accumulated from 3h, and the level of total intracellular ROS and HO-1 protein expression increased after 6h, which were significantly higher than that of the control group ( $P < 0.05$ ). These results suggested that excessive narrow-band blue light exposure can lead to intracellular and mitochondrial oxidative stress in SSRGC-5 cells.

**Dysfunction of Mitochondrial Metabolic Remodeling in SSRGC-5 Cells** Energy metabolism profile were assessed by using energy phenotype test. To determine how narrow-band blue light shifts the energy metabolism of SSRGC-5 cells, OCR was plotted as a function of ECAR in both baseline statement (rest) and stressed statement (addition of oligomycin and FCCP) to form a bioenergetic phenogram that depicts the overall energy phenotypes of the SSRGC-5 cells. The energy phenotype of cells can be described as more aerobic, energetic,

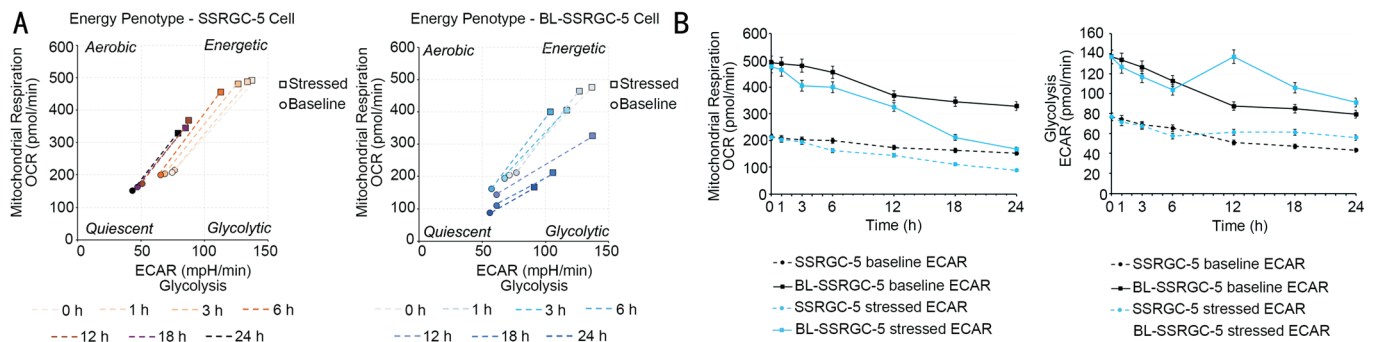


**Figure 4** Energy phenotypes of SSRGC-5 cells were assessed after narrow-band blue light exposure A: Energy phenotype of cells in the control and BL group; B: The mitochondrial respiration (baseline OCR and stressed OCR) and glycolysis (baseline ECAR and stressed ECAR) were measured between control group and BL group.

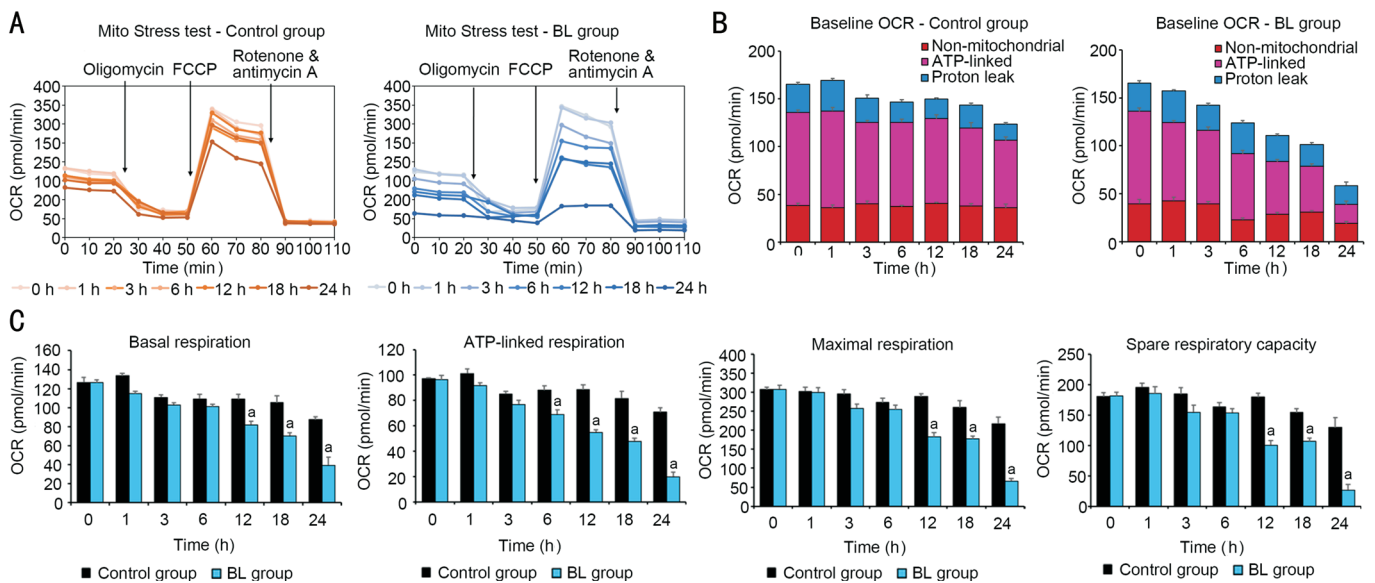


**Figure 5** Mito Stress tests were performed on SSRGC-5 cells after narrow-band blue light exposure A: In the Mito Stress tests, each data point represents 3 wells, and cellular OCRs of SSRGC-5 cells in both control and BL group were measured. Arrows point to the injection of the electron transport chain inhibitors. Oligomycin is injected after 3 basal OCR readings; next FCCP, an uncoupler, is injected, which leads to an increase in OCR; this is followed by injection with both antimycin A and rotenone, leading to inhibition of complex I and complex III of the electron transport chain. All the OCR values in different time points (0, 1, 3, 6, 12, 18, 24h) were shown as two groups, control group and BL group. B: Baseline OCR comprises non-mitochondrial respiration, proton leak-linked, and ATP-related respiration. In BL group, baseline OCR showed significant decreases caused by ATP-related respiration in a time-dependent manner compared with control group. C: The basal respiration, ATP-linked respiration, maximal respiration and spare respiratory capacity were compared between control group and BL group. <sup>a</sup>*P*<0.05.

glycolytic or quiescent. In the control group, SSRGC-5 cells exhibited a slightly shift from an energetic phenotype towards that of a Quiescent phenotype with the prolongation of culture time (Figure 4A). In contrast, narrow-band blue light induced much marked shifts towards quiescence (Figure 4A). The baseline OCR began to decline significantly after blue light exposure for 6h and was maintained at 24h (Figure 4B). In stressed cells, blue light exposure significantly reduced the OCR from 3h, and was maintained to 24h (Figure 4B). The baseline and stressed ECAR values were reduced slightly following exposure for 1, 3, and 6h (Figure 4B). With extended

exposure to blue light, the baseline and stressed ECAR values displayed a compensatory increase (Figure 4B). To further investigate a central role of mitochondrial functions in blue light-induced cellular damage, Mito Stress test analysis was used to measure mitochondrial basal oxygen consumption (respiration), ATP-linked respiration, H<sup>+</sup> (proton) leak, maximal respiration, spare respiratory capacity, and non-mitochondrial respiration. FCCP stimulated respiration in mitochondria by uncoupling ATP synthesis from electron transport, while rotenone and antimycin A inhibited complexes I and III, respectively (Figure 5A).

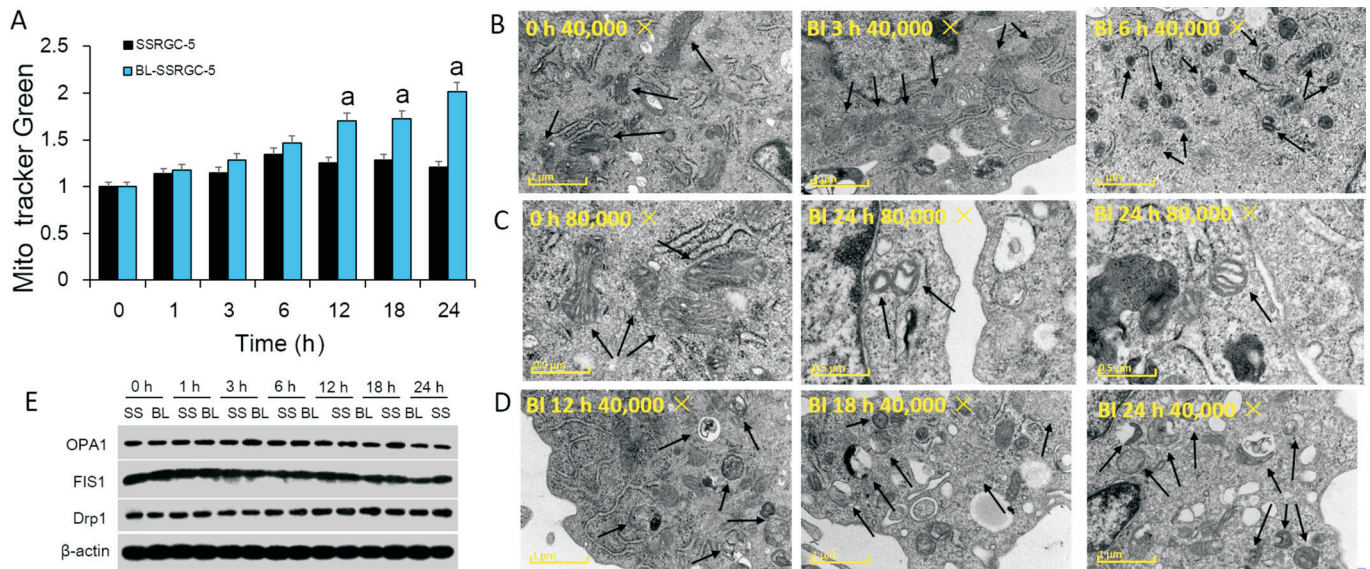


**Figure 6** Narrow-band blue light effects stimulated mitochondrial biosynthesis but impaired ultrastructure and remodeling the mitochondrial contents and ultrastructure. A: MitoTracker<sup>®</sup> Green fluorescence indicating the mitochondrial contents in BL-SSRGC-5 cells showed an increase as compared with control cells incubated in the dark. B: The number of mitochondria (arrow) in the cytoplasm of BL-SSRGC-5 cells were significantly increased, and the mitochondrial size decreased significantly. C: Compare to the normal mitochondria, the mitochondria in BL group became small, round, and displayed globular morphology. Pathological alterations related to mitochondrial matrix swelling and cristae disintegration were observed (arrows point mitochondria). D: Autophagic vacuole (arrow) increased following blue light exposure. E: Narrow-band blue light induced the up regulated expression of the mitochondrial protein OPA1, FIS1 and DRP1. <sup>a</sup>*P*<0.05.

The baseline OCR comprises non-mitochondrial respiration, proton leak-linked respiration, and ATP-related respiration. The baseline OCR in the control group declined slightly but decreased significantly in a time-dependent manner in the BL group. As Figure 5B shows, the decline in the BL group was caused mainly by a reduction in ATP-related respiration (Figure 5B, right). Basal respiration OCR were calculated by subtracting non-mitochondrial OCR from baseline OCR. It exhibited a marked decline at 12, 18, and 24h (75.34%, 66.77%, and 45.07% of the control rates, respectively; *P*<0.05; Figure 5C). Most of the basal mitochondrial OCR was dedicated to ATP-related respiration, as indicated by Oligomycin inhibition. It was significantly decreased after blue light exposure for 6, 12, 18, and 24h (78.43%, 62.04%, 58.50%, and 27.85% of the control values, respectively; *P*<0.05; Figure 5C). The remaining OCR of basal OCR was attributed to proton leakage across the membrane, which was higher at 6 h and 12h in BL-SSRGC-5 cells (*P*<0.05; Figure 5C). After injection of FCCP, all the cells showed increasing OCR values to maximal respiration rates. In BL group, the maximal respiration rates were 63.18%, 68.16%, and 30.40% at 12, 18, and 24h, respectively, of those in the control group (*P*<0.05; Figure 5C). Spare respiration capacity is an index indicates to the difference between maximal and basal respiration, and it's linked to mitochondrial fidelity. Calculations of the spare respiration capacity showed that blue light caused compromised spare respiration capacity compared

to the control group at 12, 18, and 24h (55.82%, 69.11%, and 20.48%, respectively, *P*<0.05; Figure 5C).

Collectively, the mito stress profiles of SSRGC-5 cells indicate that excessive narrow-band blue light exposure induced mitochondrial dysfunction. The alterations in mitochondrial function were consistent with the reduction in the CCK8 assay.

#### Dysregulated Mitochondrial Biosynthesis and Remodeling

A previous evidence suggests that mitochondrial biogenesis is critically involved in blue light induced injury. To illustrate the effect of long-term excessive narrow-band blue light exposure on mitochondrial biogenesis, the mitochondrial density was analyzed by Mito-Tracker green staining and flow cytometry. The mitochondrial densities of control group were increased slightly but not significantly in different times. As compared to the control cells, the mitochondrial densities of the blue light-exposed cells were significantly increased in 12, 18, and 24h, by 135.45%, 134.55%, and 166.60% of control, respectively (*P*<0.05; Figure 6A).

As semi-autonomous organelles, mitochondria are capable of changing their size and shape through consistent fusion and division. As shown in Figure 6B-6C, TEM revealed that long-term excessive narrow-band blue light exposure caused ultrastructural changes in the mitochondria of SSRGC-5 cells. Compared to those in the control condition, the number of mitochondria in the cytoplasm of BL-SSRGC-5 cells were significantly increased, and the mitochondrial size decreased significantly (Figure 6B). The mitochondria in BL-SSRGC-5

cells were small, round, and displayed globular morphology (Figure 6C). With prolonged blue light exposure, several corresponding pathological alterations related to mitochondrial matrix swelling and cristae disintegration were observed, suggesting ultrastructural damage to mitochondria undergoing dysregulated fission and fusion. Furthermore, a large number of autophagic vacuole were observed from 12h after blue light exposure, which indicates narrow-band blue light also induced autophagy activity in SSRGC-5 cells (Figure 6C).

FIS1, DRP1 and OPA1 are key proteins responsible for maintaining mitochondrial fission and fusion dynamics. As compared to the control cells, blue light significantly increased OPA1 expression at 3 and 18h exposure ( $P<0.05$ ; Figure 6E). Furthermore, blue light exposure induced significantly increase in FIS1 and DRP1 expressions especially 24h ( $P<0.05$ ; Figure 6E).

**Activation of the MAPK and AKT Pathways** To determine whether the MAPK and AKT pathways are involved in blue light-induced damage in SSRGC-5 cells, the protein expression levels of ERK, p38, JNK, phosphatidylinositol 3-kinase (PI3K), and AKT were assessed, including their phosphorylated forms (Figure 7A). Blue light exposure caused an increase in phosphorylated p38 at 3h, which was sustained at 24h. Additionally, total p38 was increased following blue light exposure for 1, 3, 6, 12, and 24h ( $P<0.05$ ). High levels of phosphorylated ERK were detected at 1h and persisted until 18h ( $P<0.05$ ); however at 24h, the expression levels in BL-SSRGC-5 cells were similar to those in unexposed SSRGC-5 cells. Moreover, no difference in total ERK expression was observed between BL-SSRGC-5 and unexposed SSRGC-5 cells. The expression of phosphorylated JNK was increased at all-time points following blue light illumination ( $P<0.05$ ), while total JNK was unaffected or weakly increased by blue light exposure.

c-Jun is an important protein in the MAPK pathway and forms the activator protein-1 (AP-1) transcription factor by heterodimerization with c-Fos. In the present study, we found that the expression levels of phosphorylated c-Jun were significantly increased at 18h following blue light exposure ( $P<0.05$ ), but at the remaining time points they were similar to the control group. However, total c-Jun was increased at all-time points ( $P<0.05$ ).

The PI3K/AKT signaling pathway is involved in diverse cellular functions including metabolism, growth, proliferation, transcription, and protein synthesis. In the present study, we found that phosphorylated PI3K was increased at 1h following blue light exposure ( $P<0.05$ ); however at the remaining time points, the levels were similar to the control group. Additionally, there was no difference in total PI3K expression between the BL-SSRGC-5 and unexposed SSRGC-5 cells.

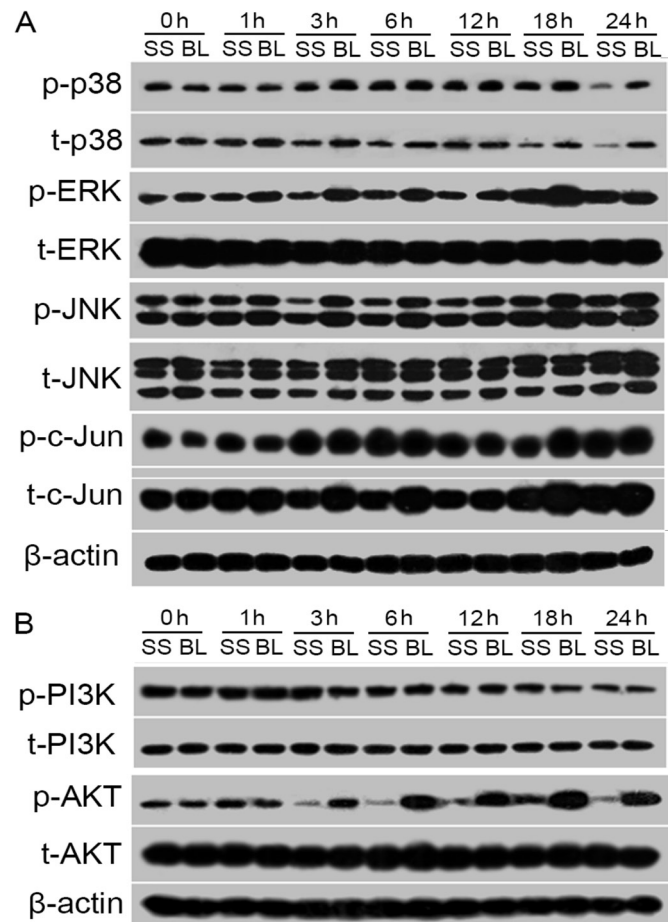


**Figure 7** Narrow-band blue light induced the expression and activation of the MAPK and AKT pathways A: Western blots showed the protein expression of p-p38, t-p38, p-ERK, t-ERK, p-JNK, t-JNK, p-c-Jun, t-c-Jun; B: p-PI3K, t-PI3K, p-AKT, t-AKT in SSRGC-5 cells and BL-SSRGC-5 cells at different time points.

Despite having no effect on PI3K expression, blue light exposure significantly increased the expression levels of phosphorylated AKT at 3h, which were sustained at 24h ( $P<0.05$ ). The expression of total AKT was similar in BL-SSRGC-5 cells and unexposed SSRGC-5 cells (Figure 7B).

Collectively, it is clear from these data that blue light triggered the activation of p38, ERK, JNK, and c-Jun in the MAPK pathways; and although the expression levels of PI3K were not affected, AKT was notably activated by blue light exposure.

## DISCUSSION

The RGC-5 cell line is a immortalized RGC line exhibiting several features of RGCs, expressing Thy-1, Brn-3c, GABA-B receptor, NMDA, and absence of glial marker GFAP expression<sup>[12-13]</sup>. But it was note that RGC-5 cells more likely represent neuronal precursor cells. Staurosporine is a kind of nonselective protein kinase inhibitor which can induce differentiation of RGC-5 cells. Differentiated RGC-5 cells are more closely resemble RGCs in morphology and physiology, such as expressing neuronal markers Thy1, microtubule-associated protein (MAP)-2, tau, and induced the development

of axon-like neurites<sup>[11,14]</sup>. Though there are still several differences between SSRGC-5 cells and primary RGCs, the SSRGC-5 cells are useful tool for studying phototoxic effect and neuronal pathophysiology for RGCs.

In the present study, we investigated the effects of excessive narrow-band blue light exposure on SSRGC-5 cells. We found that blue light damaged the axon-like structure in SSRGC-5 cells as assessed by microscopy and caused a decrease in cell viability as determined by a CCK-8 assay. However, Hoechst 33342/PI staining showed that cell death was not affected by blue light exposure. In our previous study, we confirmed that blue light induced notable apoptosis and necrosis in RGC-5 cells<sup>[10]</sup>. The difference in response to blue light damage between RGC-5 and SSRGC-5 cells is a novel observation, indicating that the immature precursor RGC-5 cells were more sensitive to blue light exposure; however, following differentiation using staurosporine, the mature SSRGC-5 cells gained resistance to blue light damage. This phenomenon highlights the importance of research focusing on whether children are more sensitive to blue light damage and how they can be protected.

The results from the CCK8 assay indicate that blue light exposure caused mitochondrial electron transport chain damage in SSRGC-5 cells; thus, we assessed the energy metabolism profiles of SSRGC-5 cells following blue light exposure. To our knowledge, this report is the first to explore energy metabolism alterations in SSRGC-5 cells after blue light exposure. The present study found a time-dependent reduction in baseline and stressed OCR in BL-SSRGC-5 cells induced by blue light exposure. Additionally, compensatory upregulation of baseline and stressed ECAR were observed at 12h following blue light exposure, which was sustained at 24h. These results indicate that blue light caused inhibition of mitochondrial respiration and increased glycolysis as compensation. The Mito Stress test further confirmed the reduction in mitochondrial respiratory function induced by blue light exposure. The basal, ATP-related, and maximal respiration, and spare respiratory capacity were depleted in BL-SSRGC-5 cells as compared with unexposed SSRGC-5 cells. This is consistent with the reduction in BL-SSRGC-5 cell viability following blue light exposure.

The inhibition of mitochondrial function may be caused by a reduction in mitochondrial contents or mitochondrial dysfunction. We found that the mitochondrial contents were significantly increased following blue light exposure; thus, to further evaluate the damage at the organelle level, we performed TEM to observe changes in the ultrastructure. The results show that there was an imbalance in mitochondrial fission and fusion following blue light exposure, and the mitochondria became small and round with cristae alterations.

With increasing exposure time, the mitochondrial contents were increased, especially in the axon-like structures, and more mitochondria showed pathological changes such as matrix swelling and cristae disintegration.

Mitochondrial fusion events are mediated by mitochondrial proteins including Mfn1, Mfn2, and OPA1<sup>[15]</sup>, and it has been shown that Drp1 and FIS1 are crucial components of the mitochondrial fission process<sup>[16]</sup>. In the present study, we found that OPA1 expression was upregulated in BL-SSRGC-5 cells at 3 and 18h following blue light exposure, and Drp1 and FIS1 expression levels were increased at 24h following blue light exposure. The results suggests that narrow-band blue light caused SSRGC-5 cells displayed mitochondrial abnormalities in function, contents and structure, which were associated with the dysregulated remodeling of mitochondria *via* relative proteins.

Previous studies have reported that ROS generation is involved in the ultraviolet and white light exposure process in RGC-5 cells<sup>[17-18]</sup>. Our previous study found that blue light exposure can trigger an increase in intracellular ROS levels in RGC-5 cells following blue light exposure 14 and 22h<sup>[10]</sup>. In the present study, we used two different fluorescent probes, DCFH-DA and MitoSox<sup>TM</sup> Red, to separately detect intracellular ROS and superoxide generated in mitochondria in BL-SSRGC-5 and unexposed SSRGC-5 cells at different time points. The results suggest that both the intracellular ROS and superoxide levels were significantly enhanced following blue light exposure, which is consistent with previous studies. Additionally, the ROS-sensitive protein, HO-1, was increased in BL-SSRGC-5 cells at 6h following blue light exposure, which was sustained at 24h. HO-1 has been reported to play an important role as a potent antioxidant and anti-inflammatory protein that maintains cellular homeostasis. The present results are consistent with previous observations in RGC-5 cells exposed to white, blue, and ultraviolet light<sup>[10,18-19]</sup>, which demonstrate that blue light damage caused oxidative stress in both RGC-5 and SSRGC-5 cells.

The MAPKs regulate diverse cellular functions by converting extracellular signals into intracellular responses<sup>[20]</sup> such as cell growth, differentiation, inflammation, and cell death<sup>[21]</sup>. The MAPKs in mammalian cells belong to three subgroups; the extracellular signal regulated kinases (ERK), the c-Jun N-terminal kinases (JNK), and the p38 kinases<sup>[22]</sup>. ERK activation contributes to cell differentiation, proliferation and survival. JNK and p38 are related to inflammatory and environmental stress and apoptosis.

ROS have been demonstrated to induce or mediate the activation of the MAPK pathways, and numerous studies have shown that cellular stimuli that induce ROS production also activate the MAPK pathways in various cell types<sup>[23]</sup>. In

the present study, we found that ERK, JNK and c-Jun were persistently activated following blue light exposure, and p38 was activated at 3 and 18h. It suggests that MAPKs triggered by oxidative stress were widely involved in blue light-induced damage in SSRGC-5 cells. However, in our previous study in RGC-5 cells, blue light illumination caused remarkable cell apoptosis from 14h and blue light induced the persistent activation of p38 and JNK pathways at 1, 2, 14, and 22h, and activated the ERK pathway at the early time periods. In contrast, the death rates were no differ in SSRGC-5 cells between BL group and controls in this study. This results suggest the persistent activation of ERK played an important role in promote SSRGC-5 survival from excessive narrow-band blue light.

The AKT pathway is a key signaling molecule in diverse biological processes including cell proliferation, growth, and survival<sup>[24]</sup>. AKT could protect RPE cells from oxidant-induced cell death in normal and disease states<sup>[25]</sup>. The decline of phosphorylated AKT might contribute to RPE cell dysfunction<sup>[26]</sup>. It has been demonstrated that mitochondrial fission plays an important role in ROS production in cardiovascular and human hepatocellular carcinoma cells. Elevated ROS inhibit cell apoptosis by activating the AKT pathway and promoting global autophagy. Moreover, activation of AKT has been shown to be associated with enhanced glycolysis in cancer cells<sup>[27]</sup>. In the present study, SSRGC-5 cells displayed a higher resistance to blue light exposure than RGC-5 cells, which may have contributed to the general autophagy as confirmed by TEM. The autophagy cleared the dysfunctional mitochondria and promoted ROS production, which activated AKT expression and promoted cell survival. Furthermore, blue light exposure damaged mitochondrial respiration and the AKT pathway promoted glycolysis as a compensatory measure to meet the energy demands.

Taken together, narrow-band blue light damaged SSRGC-5 cells by targeting mitochondria. The mitochondria underwent dysregulated remodeling, which were accompanied by oxidative stress. The ROS generation triggered the MAPK and AKT signaling pathways, which involved in the potential mechanism to protect SSRGC-5 cells from death in a compromised state. Considering the fact that RGC-5 cells do not fully simulate RGCs *in vivo*, we need to further clarify and study the blue light effect *in vivo* with better model. However, this study provides a novel mechanism of blue light damage in RGC-5 cells, which may provide potential target for protecting retinal neurons especially RGCs and preventing further damage of visual ability.

#### ACKNOWLEDGEMENTS

**Foundations:** Supported by the National Natural Science Foundation of China (No.81670821; No.81400440).

**Conflicts of Interest:** Guo KX, None; Huang C, None; Wang W, None; Zhang P, None; Li Y, None; Liu ZY, None; Wang MS, None.

#### REFERENCES

- 1 Mainster MA. Violet and blue light blocking intraocular lenses: photoprotection versus photoreception. *Br J Ophthalmol* 2006;90(6): 784-792.
- 2 Bennet D, Kim MG, Kim S. Light-induced anatomical alterations in retinal cells. *Anal Biochem* 2013;436(2):84-92.
- 3 Olmo-Aguado S, Núñez-Álvarez C, Osborne NN. Blue light action on mitochondria leads to cell death by necroptosis. *Neurochem Res* 2016;41(9):2324-2335.
- 4 Lascaratos G, Ji D, Wood JPM, Osborne NN. Visible light affects mitochondrial function and induces neuronal death in retinal cell cultures. *Vis Res* 2007;47(9):1191-1201.
- 5 Alaimo A, Liñares GG, Bujjamer JM, Gorojod RM, Alcon SP, Martínez JH, Baldessari A, Grecco HE, Kotler ML. Toxicity of blue led light and A2E is associated to mitochondrial dynamics impairment in ARPE-19 cells: implications for age-related macular degeneration. *Arch Toxicol* 2019;93(5):1401-1415.
- 6 Chhetri J, Gueven N. Targeting mitochondrial function to protect against vision loss. *Expert Opin Ther Targets* 2016;20(6):721-736.
- 7 Kalyanaraman B, Cheng G, Hardy M, Ouari O, Lopez M, Joseph J, Zielonka J, Dwinell MB. A review of the basics of mitochondrial bioenergetics, metabolism, and related signaling pathways in cancer cells: Therapeutic targeting of tumor mitochondria with lipophilic cationic compounds. *Redox Biol* 2018;14:316-327.
- 8 Osborne NN, Núñez-Álvarez C, del Olmo-Aguado S. The effect of visual blue light on mitochondrial function associated with retinal ganglions cells. *Exp Eye Res* 2014;128:8-14.
- 9 Xie C, Yi J, Lu J, Nie MW, Huang MF, Rong JF, Zhu ZH, Chen J, Zhou XL, Li BM, Chen HM, Lu NH, Shu X. *N*-acetylcysteine reduces ROS-mediated oxidative DNA damage and PI3K/Akt pathway activation induced by *Helicobacter pylori* infection. *Oxidative Med Cell Longev* 2018;2018:1874985.
- 10 Huang C, Zhang P, Wang W, Xu YS, Wang MS, Chen XY, Dong XR. Long-term blue light exposure induces RGC-5 cell death *in vitro*: involvement of mitochondria-dependent apoptosis, oxidative stress, and MAPK signaling pathways. *Apoptosis* 2014;19(6):922-932.
- 11 Zhang P, Huang C, Wang W, Wang MS. Early changes in staurosporine-induced differentiated RGC-5 cells indicate cellular injury response to nonlethal blue light exposure. *Photochem Photobiol Sci* 2015;14(6):1093-1099.
- 12 Tian SW, Ren Y, Pei JZ, Ren BC, He Y. Pigment epithelium-derived factor protects retinal ganglion cells from hypoxia-induced apoptosis by preventing mitochondrial dysfunction. *Int J Ophthalmol* 2017;10(7):1046-1054.
- 13 Wang WJ, Jin W, Yang AH, Chen Z, Xing YQ. Protective effects of ciliary neurotrophic factor on the retinal ganglion cells by injure of hydrogen peroxide. *Int J Ophthalmol* 2018;11(6):923-928.

- 14 Ganapathy PS, Dun Y, Ha Y, Duplantier J, Allen JB, Farooq A, Bozard BR, Smith SB. Sensitivity of staurosporine-induced differentiated RGC-5 cells to homocysteine. *Curr Eye Res* 2010;35(1):80-90.
- 15 Zemirli N, Morel E, Molino D. Mitochondrial dynamics in basal and stressful conditions. *Int J Mol Sci* 2018;19(2):564.
- 16 Kim H, Scimia MC, Wilkinson D, Trelles RD, Wood MR, Bowtell D, Dillin A, Mercola M, Ronai ZA. Fine-tuning of Drp1/Fis1 availability by AKAP121/Siah2 regulates mitochondrial adaptation to hypoxia. *Mol Cell* 2011;44(4):532-544.
- 17 Li GY, Osborne NN. Oxidative-induced apoptosis in an immortalized ganglion cell line is caspase independent but involves the activation of poly(ADP-ribose)polymerase and apoptosis-inducing factor. *Brain Res* 2008;1188:35-43.
- 18 Ji D, Kamalden TA, Olmo-Aguado S, Osborne NN. Light- and sodium azide-induced death of RGC-5 cells in culture occurs via different mechanisms. *Apoptosis* 2011;16(4):425-437.
- 19 Balaiya S, Murthy RK, Brar VS, Chalam KV. Evaluation of ultraviolet light toxicity on cultured retinal pigment epithelial and retinal ganglion cells. *Clin Ophthalmol* 2010;4:33-39.
- 20 Cargnello M, Roux PP. Activation and function of the MAPKs and their substrates, the MAPK-activated protein kinases. *Microbiol Mol Biol R* 2011;75(1):50-83.
- 21 Junttila MR, Li SP, Westermarck J. Phosphatase-mediated crosstalk between MAPK signaling pathways in the regulation of cell survival. *FASEB J* 2008;22(4):954-965.
- 22 Son Y, Cheong YK, Kim NH, Chung HT, Kang DG, Pae HO. Mitogen-activated protein kinases and reactive oxygen species: how can ROS activate MAPK pathways? *J Signal Transduct* 2011;2011:792639.
- 23 McCubrey JA, LaHair MM, Franklin RA. Reactive oxygen species-induced activation of the MAP kinase signaling pathways. *Antioxid Redox Signal* 2006;8(9-10):1775-1789.
- 24 Mayer IA, Arteaga CL. The PI3K/AKT pathway as a target for cancer treatment. *Annu Rev Med* 2016;67:11-28.
- 25 Gong YQ, Huang W, Li KR, Liu YY, Cao GF, Cao C, Jiang Q. SC79 protects retinal pigment epithelium cells from UV radiation via activating Akt-Nrf2 signaling. *Oncotarget* 2016;7(37):60123-60132.
- 26 Chen XD, Su MY, Chen TT, Hong HY, Han AD, Li WS. Oxidative stress affects retinal pigment epithelial cell survival through epidermal growth factor receptor/AKT signaling pathway. *Int J Ophthalmol* 2017;10(4):507-514.
- 27 Elstrom RL, Bauer DE, Buzzai M, Karnauskas R, Harris MH, Plas DR, Zhuang HM, Cinalli RM, Alavi A, Rudin CM, Thompson CB. Akt stimulates aerobic glycolysis in cancer cells. *Cancer Res* 2004;64(11):3892-3899.